Activity-Dependent Plasticity of Descending Synaptic Inputs to Spinal Motoneurons in an *In Vitro* Turtle Brainstem–Spinal Cord Preparation

Stephen M. Johnson and Gordon S. Mitchell

Department of Comparative Biosciences, School of Veterinary Medicine, University of Wisconsin, Madison, Wisconsin 53706

An *in vitro* brainstem–spinal cord preparation from adult turtles was used to test the hypothesis that descending synaptic inputs to multifunctional spinal motoneurons (i.e., involved in respiration and locomotion) express activity-dependent depression or potentiation. The tissue was placed in a chamber that allowed for separate superfusion of the brainstem, spinal segments C_2–C_4, and C_5–D_1. Action potential conduction between the brainstem and spinal segments C_5–D_1 was blocked by superfusing C_2–C_4 with Na^+-free solution. With C_5–D_1 at $[K^+] = 10$ mM, electrical stimulation at C_5 every 2 min evoked potentials in intact pectoralis (expiratory, inward rotation of shoulder) and serratus (inspiratory, outward rotation of shoulder) nerves that were stable for at least 2 hr. Application of conditioning stimulation (900 pulses at 1 or 10 Hz) at C_5 decreased pectoralis evoked potential amplitudes by ~40% initially and by 20% after 90 min; serratus evoked potentials were unaltered. Conditioning stimulation (100 Hz, 900 pulses) transiently depressed pectoralis evoked potential amplitude by <20% but produced a delayed 72% increase in serratus evoked potential amplitude after ~80 min. Conditioning stimulation (10 Hz) at C_5 also reduced the amplitude of sensory afferent evoked potentials in pectoralis produced by stimulating ipsilateral dorsal roots at C_8. Thus, long-lasting changes in descending synaptic inputs to multifunctional spinal motoneurons were frequency-dependent and heterosynaptic. We hypothesize that activity-dependent plasticity may modulate descending synaptic drive to spinal motoneurons involved in both respiration and locomotion.

Key words: respiration; breathing; locomotion; LTP; LTD; motor control

Central neural networks subserving motor behaviors, such as respiration and locomotion, must be flexible and optimize their motor output in response to a variety of changing physiological conditions, as well as in response to disease and injury. The degree of plasticity (i.e., ability to alter future performance based on experience) that can be expressed within these motor neural circuits, particularly at the level of the spinal cord, is of great interest and has been reviewed with respect to respiration (McCrimmon et al., 1995; Powell et al., 1998) and locomotion (Durkovic, 1986; Hodgson et al., 1994; Muir and Steeves, 1997) (also see Carrier et al., 1997). The cellular and synaptic mechanisms underlying spinal plasticity are, however, not well understood.

Activity-dependent plasticity can be defined as a change in the translation of synaptic input into action potential firing (i.e., synaptic efficacy) as a result of previous synaptic activity. Two well known forms of activity-dependent plasticity are long-term depression (LTD) and long-term potentiation (LTP). LTD is a long-lasting (>1 hr) decrease in synaptic efficacy caused by low-frequency (0.5–3 Hz) stimulation of synaptic pathways (for review, see Linden, 1994; Zhuo and Hawkins, 1995; Bear and Abraham 1996). In contrast, LTP is a long-lasting (>1 hr) increase in synaptic efficacy caused by high-frequency (40–100 Hz) stimulation of synaptic pathways (for review, see Bliss and Collingridge 1993). LTD and LTP are found in many parts of the nervous system, and it is possible that these forms of activity-dependent plasticity may contribute to spinal plasticity.

To test whether activity-dependent plasticity is expressed in descending pathways to identified spinal motoneurons involved in both respiration and locomotion, an *in vitro* brainstem–spinal cord preparation from adult, semiaquatic turtles was used. This *in vitro* preparation is derived from a fully mature vertebrate and produces appropriate expiratory and inspiratory motor activity on intact nerves (Johnson and Mitchell, 1998a). For respiration, turtles generate positive and negative air pressures in their lungs by alternately moving their pliable soft tissue pectoral and pelvic girdles inward (expiration) and outward (inspiration). For the rostrally located pectoral girdle, the primary respiratory muscles are the pectoralis (expiratory) and serratus (inspiratory) muscles (Gans and Hughes, 1967; Takeda et al., 1986). During swimming and walking, pectoralis and serratus muscles likely contribute to inward and outward rotation of the shoulder, respectively, in a manner similar to the equivalent respiratory–locomotor motoneurons in the turtle lumbar spinal cord that control the pelvic girdle and hip movement (Stein et al., 1998). In this study, descending synaptic inputs to multifunctional pectoralis and serratus motoneurons in an isolated turtle brainstem–spinal cord preparation were electrically stimulated at various frequencies to test for activity-dependent plasticity.

A preliminary report of this work was published in abstract form (Johnson and Mitchell, 1998b).
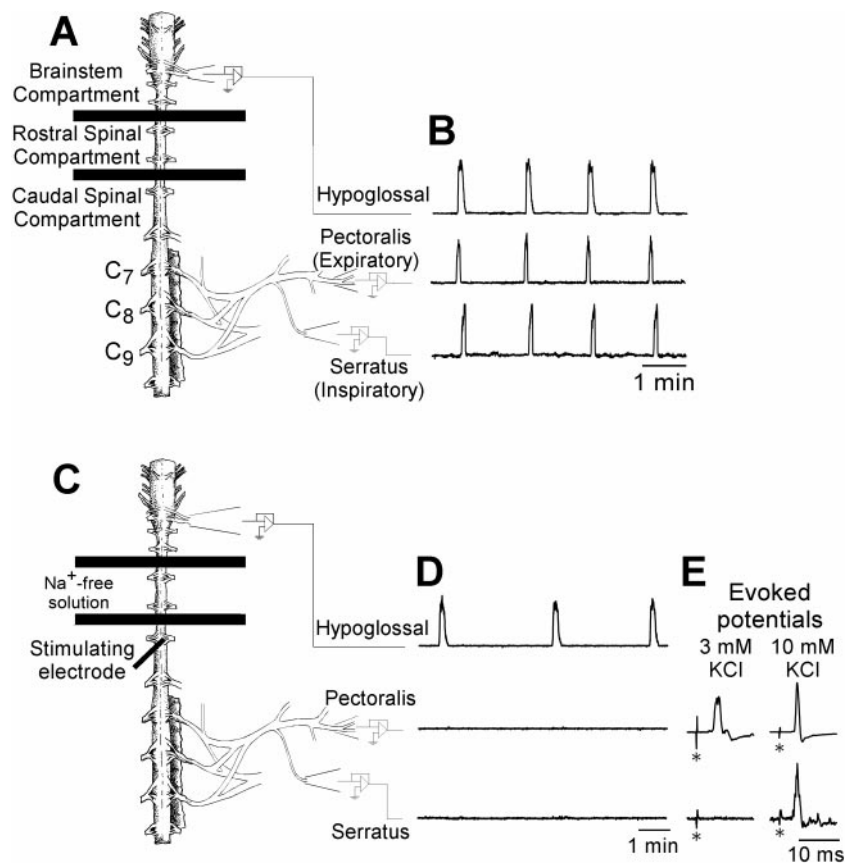
Figure 1. Spontaneous respiratory motor activity and electrically evoked potentials produced by turtle brainstem-spinal cord preparations. *A, C,* Drawings of turtle brainstem–spinal cord preparations are shown with barriers between C_2 and C_3 and between C_4 and C_5, which establish the brainstem compartment, rostral spinal compartment, and caudal spinal compartment. *B,* Suction electrodes attached to hypoglossal nerve rootlets and intact pectoralis and serratus nerves record rhythmic, synchronized spontaneous respiratory motor activity. The integrated traces (time constant, 200 msec) are shown for each nerve. *C,* Schematic drawing of the turtle brainstem–spinal cord preparation with Na^+-free solution flowing into the rostral spinal cord compartment, resulting in a blockade of action potential conduction between the brainstem and spinal cord. *D,* Under these conditions, suction electrodes attached to hypoglossal nerve rootlets record rhythmic, spontaneous respiratory activity, whereas electrodes attached to pectoralis and serratus nerves record no respiratory activity. *E,* A metal electrode inserted into the spinal cord at C_5 ipsilateral to the intact pectoralis and serratus nerves (*dark heavy line* in *C*) was used to electrically stimulate descending synaptic inputs to pectoralis and serratus spinal motoneurons (stimulus artifacts marked with *asterisks*). Evoked potentials were typically observed in pectoralis, but not serratus, nerves when the caudal spinal compartment $[K^+]$ was 3 mM (*left traces*). When the caudal spinal compartment $[K^+]$ was 10 mM (*right traces*), pectoralis evoked potentials were larger (stimulus artifacts in both pectoralis traces are the same absolute size; the gain on the *left trace* is 5 times larger than that on the *right trace*), and evoked potentials appeared on serratus.

MATERIALS AND METHODS

Turtle brainstem–spinal cord preparation. Adult turtles (*Pseudemys scripta*, $n = 41$, 610 ± 30 gm) were obtained from commercial suppliers and kept in a large open tank where they had access to water for swimming and heat lamps and dry areas for basking. The isolation of the brainstem and spinal cord was performed as described previously (Johnson and Mitchell, 1998a). Briefly, turtles were intubated and anesthetized with 4% halothane in 100% O_2 until the limb withdrawal reflex to noxious foot pinch was eliminated. The plastron was rapidly removed, and the ascending aorta was perfused with oxygenated (1.2–1.3% CO_2, balance O_2) standard solution at 22°C for 1–2 min. The composition of standard solution was (in mM): 100 NaCl, 23 NaHCO$_3$, 10 glucose, 2.5 CaCl$_2$, 2.5 MgCl$_2$, 1.0 K$_2$PO$_4$, and 1.0 KCl. The bone and muscle covering the dorsal surface of the brainstem and spinal cord were removed, and the remaining tissue was submerged in oxygenated standard solution at 22°C. All brain tissue rostral to the optic lobes was removed, and all bone and muscle surrounding the brainstem and spinal cord were removed with the pectoralis and serratus nerves isolated and left intact on one side of the spinal cord. The spinal column from C_7–D_1 ipsilateral to the pectoralis and serratus nerves was left intact (Fig. 1*A,C*). The tissue was pinned down (ventral surface upward) in a recording chamber that was split into three compartments by partitions made of plastic and petroleum jelly. The brainstem compartment (~25 ml volume) contained the brainstem and spinal cord down to C_2; the rostral spinal compartment (~8 ml volume) contained spinal segments C_3–C_4; and the caudal spinal compartment (~35 ml volume) contained spinal segments C_5–D_1.

After establishing the three compartments, fluid flowing into the brainstem compartment was switched to a solution containing HEPES buffer as follows (in mM): 100 NaCl, 23 NaHCO$_3$, 10 glucose, 5 HEPES (sodium salt), 5 HEPES (free acid), 2.5 CaCl$_2$, 2.5 MgCl$_2$, 1.0 K$_2$PO$_4$, and 1.0 KCl (for justifying use of HEPES buffer, see Johnson and Mitchell, 1998a). The HEPES solution was bubbled with 5% CO_2 and 95% O_2 and flowed into the brainstem compartment (2–4 ml/min), whereas standard solution bubbled with 1.2% CO_2 and balance O_2 flowed into the two spinal compartments (2–4 ml/min). The pH in the brainstem compartment and caudal spinal compartment was periodically monitored with a calomel glass pH electrode (Digi-Sense; Cole-Parmer,

Vernon Hills, IL). The pH of the brainstem compartment was maintained at 7.40 ± 0.1, and the caudal spinal compartment was maintained at 7.95 ± 0.1 (for justification of pH values, see Johnson and Mitchell, 1998a).

Immediately after attaching recording electrodes, preparations were allowed to equilibrate for 1–2 hr before allowing Na^+-free solution to flow into the rostral spinal compartment and to block action potential conduction between the brainstem and the caudal spinal cord (Fig. 1*C*). The Na^+-free solution was bubbled with 1.2% CO_2 and balance O_2, and its composition was as follows (in mM): 100 choline chloride ($C_5H_{14}NO\cdot Cl$), 23 choline bicarbonate (i.e., 8.45 ml of 45% solution of $C_5H_{14}NO\cdot HCO_3$/l), 10 glucose, 2.5 CaCl$_2$, 2.5 MgCl$_2$, and 3.0 KCl. Na^+-free solution flowed initially at ~30 ml/min for 5 min and then at a maintenance rate of 1–2 ml/min. Although rhythmic respiratory activity on pectoralis and serratus nerves (Fig. 1*B*) was abolished in 45–60 min (Fig. 1*D*), experimental protocols were not started until at least 60 min after switching to Na^+-free solution.

Nerve recording and electrical stimulation. To record electrically evoked potentials, glass suction electrodes were attached to the cut free ends of pectoralis and serratus nerves (Figs. 1*A,C*). The signals were amplified ($10,000\times$) and bandpass-filtered (10–10,000 Hz) using a differential AC amplifier (model 1700; A-M Systems, Carlsborg, WA) before being digitized and analyzed using pClamp software (Axon Instruments, Foster City, CA). Evoked potentials were obtained by electrically stimulating the ipsilateral spinal cord at C_5 with tungsten or stainless steel electrodes (5 MΩ; A-M Systems) (Fig. 1*E*). Optimal evoked potentials were obtained by inserting the stimulating electrodes into the ventral surface of the spinal cord, approximately halfway between the midline and the lateral margin at a depth of 500–700 μm (Fig. 2*A*).

Baseline data for pectoralis and serratus evoked potentials were obtained by applying test stimuli (400–500 μA of negative current, 0.2–0.5 msec duration) every 2 min for 10–20 min. To test for activity-dependent changes in the evoked potentials, conditioning stimulation (900 pulses at same intensity as test stimuli) was applied at 1, 10, or 100 Hz. Test stimuli were then applied every 2 min to determine the effects of the conditioning stimulation. Only one bout of conditioning stimulation was applied in each experiment. Evoked potentials caused by activating ipsilateral spi-

nal sensory afferent inputs were obtained by attaching a suction electrode to cut dorsal spinal roots at C_8 (cut was proximal to the dorsal root ganglion) and applying test stimuli (400–500 μA of positive current, 0.2 msec duration) every 4 min.

Data analysis and statistics. Evoked potential amplitude was measured in arbitrary units and normalized to the average of the baseline data obtained during the first 10–20 min of applied test stimuli. Onset latency was measured from the beginning of the stimulus artifact to the start of the initial upward portion of the evoked potential. Peak latency was measured from the onset of the stimulus artifact to the largest positive deflection in the evoked potential. All measurements were reported as the mean ± SEM. For statistical inferences, data were pooled together in 10 min bins (10, 20, or 60 min bins were used for baseline data), and two statistical tests were performed for each set of control data and data obtained with conditioning stimulation. A one-way ANOVA with repeated measures design was used to ask whether any data in the bins were different from the baseline data. A two-way ANOVA with repeated measures design was used to ask whether the data from the control group (no conditioning stimulation applied) differed from the data from the group with conditioning stimulation. The two-way ANOVA takes into account the total variance in both groups and determines whether there are effects attributable to time (i.e., presence of a slope), conditioning stimulation (i.e., upward or downward shift), or a time–conditioning interaction (i.e., slope change). *Post hoc* comparisons were performed using the Bonferroni test (Sigma Stat; Jandel Scientific Software, San Rafael, CA). *p* values < 0.05 were considered significant.

RESULTS

Properties of pectoralis and serratus evoked potentials from descending inputs

When the caudal spinal compartment was bathed with standard solution ($[K^+]$ = 3 mM) and test stimuli were applied, pectoralis evoked potentials with a single large peak were commonly observed. In contrast, serratus evoked potentials had a very small, irregular amplitude (Figs. 1*E, left traces*, 3*A*). At $[K^+]$ = 3 mM, the onset latency and peak latency for the pectoralis evoked potentials were 4.3 ± 0.1 and 7.0 ± 0.2 msec, respectively (*n* = 12) (serratus was not measured). When the $[K^+]$ in the caudal spinal compartment was increased to 10 mM, pectoralis evoked potential amplitude increased by ~300% (Figs. 1*E, right traces*, 2*B*), whereas the onset latency and peak latency were relatively unchanged (4.9 ± 0.2 and 6.9 ± 0.2 msec, respectively; *n* = 29). Measurable serratus evoked potentials appeared within 10 min of increasing $[K^+]$ and increased in amplitude to maximal values during the next 40 min (Fig. 2*B*). Because the largest evoked potentials were obtained 50–60 min after the switch from 3 to 10 mM $[K^+]$, at least 1 hr was allowed between the time of the switch and the beginning of data collection. At $[K^+]$ = 10 mM, the onset latency and peak latency for serratus evoked potentials were 5.0 ± 0.1 and 6.3 ± 0.2 msec, respectively. These data suggest that serratus motoneurons may be hyperpolarized, have a larger rheobase, or have less excitatory synaptic current compared with pectoralis motoneurons. Unless noted otherwise, the $[K^+]$ in the caudal spinal compartment was routinely increased to 10 mM to produce both pectoralis and serratus evoked potentials. In several experiments (*n* = 8), evoked potential amplitude versus current intensity plots were produced by varying the stimulus intensity. Pectoralis and serratus evoked potentials were first observed at 50 μA and increased rapidly in size between 50 and 300 μA before leveling off at 400–500 μA (Fig. 2*C*). Thus, most test stimuli and conditioning stimuli were applied at 400–500 μA to reduce variability and avoid tissue damage.

Activity-dependent changes in evoked potentials from descending inputs

With $[K^+]$ at 3 mM in the caudal spinal compartment, test stimuli applied every 2 min produced evoked potentials in pectoralis
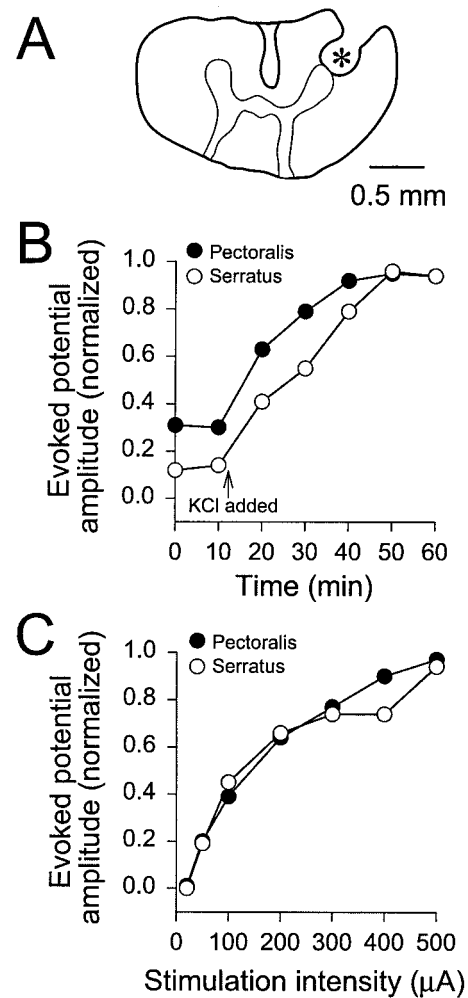

Figure 2. Stimulating electrode location, time-dependent effects of increased $[K^+]$, and stimulus–potential curves. *A*, Camera lucida drawing of a transverse section of spinal cord at C_5 showing the location of an electrolytic lesion in the ventral spinal cord produced by the metal stimulating electrode (marked with an *asterisk*). The tissue was fixed, frozen, and cut into 100-μm-thick sections before mounting on slides. No correction was made for tissue shrinkage in the scale bar. *B*, Time-dependent effects of increasing $[K^+]$ in the caudal spinal compartment from 3 to 10 mM. Test stimuli (400 μA, 0.2 msec duration) were applied every 10 min with $[K^+]$ at 3 mM, and then KCl was added to make $[K^+]$ 10 mM (indicated by the *arrow*; *n* = 11). The evoked potential amplitudes were measured in arbitrary units and normalized to the largest amplitude within each data set. Both pectoralis and serratus reached maximal amplitude levels after 50–60 min. *C*, Stimulus–potential curves for pectoralis and serratus evoked potentials when the caudal spinal $[K^+]$ was 10 mM. Amplitudes were measured in arbitrary units and normalized to the largest amplitude within each data set (usually 500 μA).

whose amplitude was unaltered for at least 2 hr (*n* = 6; Fig. 3*A,C*). There was little change in peak latency of the pectoralis evoked potentials for ~80 min, and then they became more variable (*p* > 0.05; Fig. 3*D*). Serratus evoked potentials were often not observed or were small and highly variable. Therefore, serratus evoked potentials were not measured. After 1 Hz conditioning stimulation (900 pulses) had been applied to the spinal cord (*n* = 6), pectoralis evoked potential amplitude was decreased immediately by 40% relative to baseline and relaxed toward a plateau that was 20% less than baseline ~80 min after conditioning stimulation (*p* < 0.05; Fig. 3*B,C*). After averaging the amplitude data in 10
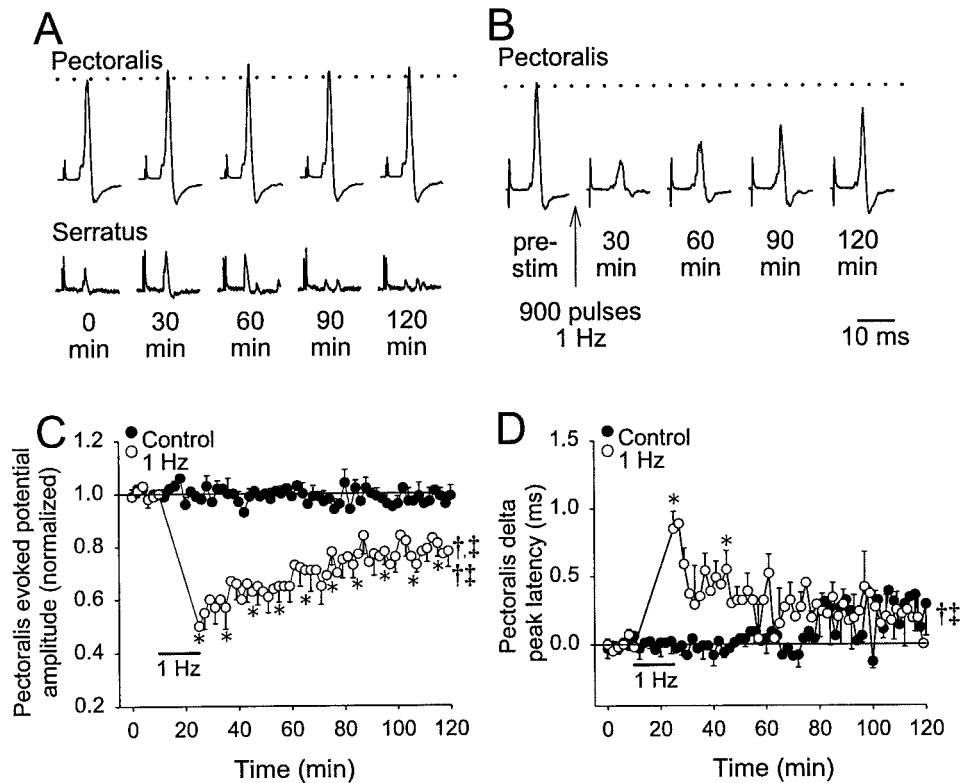
Figure 3. One hertz conditioning stimulation at [K$^+$] = 3 mM. *A*, Evoked potentials shown for pectoralis (*top traces*) and serratus (*bottom traces*) are shown at the times indicated below. Test stimuli were applied every 2 min for 2 hr. The *dotted line* shows the average amplitude for the traces obtained in the first 10 min (stimulus artifacts are truncated). *B*, Pectoralis evoked potentials are shown from an experiment in which 1 Hz conditioning stimulation (900 pulses, 0.2 msec duration, 400 μA) was applied at the time indicated by the *vertical arrow*. Serratus evoked potentials at [K$^+$] = 3 mM were absent or extremely small. *C*, Population data for the pectoralis evoked potential amplitudes with respect to time are shown. The control data in which only test stimuli were applied are indicated by the *solid circles* (*n* = 6), whereas the data in which 1 Hz conditioning stimulation was applied are indicated by the *open circles* (*n* = 6). The labeled *solid bar* shows the time during which 1 Hz conditioning stimulation was applied. *D*, Population data for the change in peak latency of pectoralis evoked potentials are graphed as the change from the average during the first 10 min (*solid line* at *0.0*). For statistical purposes, data were pooled together in 10 min bins and averaged. A repeated measures one-way ANOVA was performed to compare all time points to baseline (i.e., the first 10 min); significance is indicated by *asterisks*. Two-way ANOVA results are indicated by *symbols* (†, time; ‡, conditioning stimulation; †‡, time–conditioning stimulation interaction).

min bins, all time points after 1 Hz conditioning stimulation were significantly decreased from baseline. A two-way ANOVA with repeated measures design indicated that 1 Hz conditioning stimulation elicited a response significantly different from control experiments through effects of time, conditioning stimulation, and a time–conditioning interaction. Pectoralis peak latency increased by almost 1.0 msec above baseline during the first 2 min after conditioning stimulation, recovered to 0.3–0.5 msec above baseline within the next 30–40 min, and gradually decreased toward, but not to, baseline levels after 110 min (Fig. 3*D*). Only two individual 10 min bins were significantly different from baseline after 1 Hz conditioning stimulation; these effects were significant as a time–conditioning interaction.

With [K$^+$] at 10 mM in the caudal spinal compartment, test stimuli produced evoked potentials in both pectoralis and serratus nerves whose amplitude was relatively unaltered for at least 2 hr (*n* = 6; Fig. 4*A,C,E*). The amplitude of serratus evoked potentials was still more variable than pectoralis when test stimuli were applied (Fig. 4*A,C,E*). However, pectoralis peak latency increased slowly with time at a rate of ~0.25 msec/hr (*p* < 0.05; Fig. 4*D*), whereas serratus peak latency was relatively unchanged for 60 min before becoming more variable (*p* > 0.05; Fig. 4*F*). After 1 Hz conditioning stimulation had been applied (*n* = 8),

pectoralis evoked potential amplitude decreased initially by ~36% relative to baseline and remained decreased by at least 18% for another 115 min (Fig. 4*B,C*). All data in 10 min bins after 1 Hz conditioning stimulation were significantly decreased from baseline, and significant time, conditioning stimulation, and time–conditioning stimulation interactions were revealed when compared with control experiments. In contrast, mean serratus evoked potential amplitude increased steadily for 60 min after 1 Hz conditioning stimulation by ~40% (Fig. 4*E*); however, this large increase was attributable to effects in only three of eight preparations (one example is shown in Fig. 4*B, bottom trace*). Although significant in a one-way ANOVA (*p* < 0.05), none of the individual time points was significantly greater than baseline, and no significant differences from control experiments were revealed by a two-way ANOVA. Both pectoralis and serratus peak latencies increased (~1.0 and 0.6–0.8 msec, respectively) immediately after 1 Hz conditioning stimulation, although only the pectoralis data reached statistical significance (Fig. 4*D,F*). Pectoralis peak latency after conditioning stimulation was significantly different from control for time, conditioning stimulation, and a time–conditioning stimulation interaction, whereas serratus peak latency was significant only for the time–conditioning stimulation interaction.
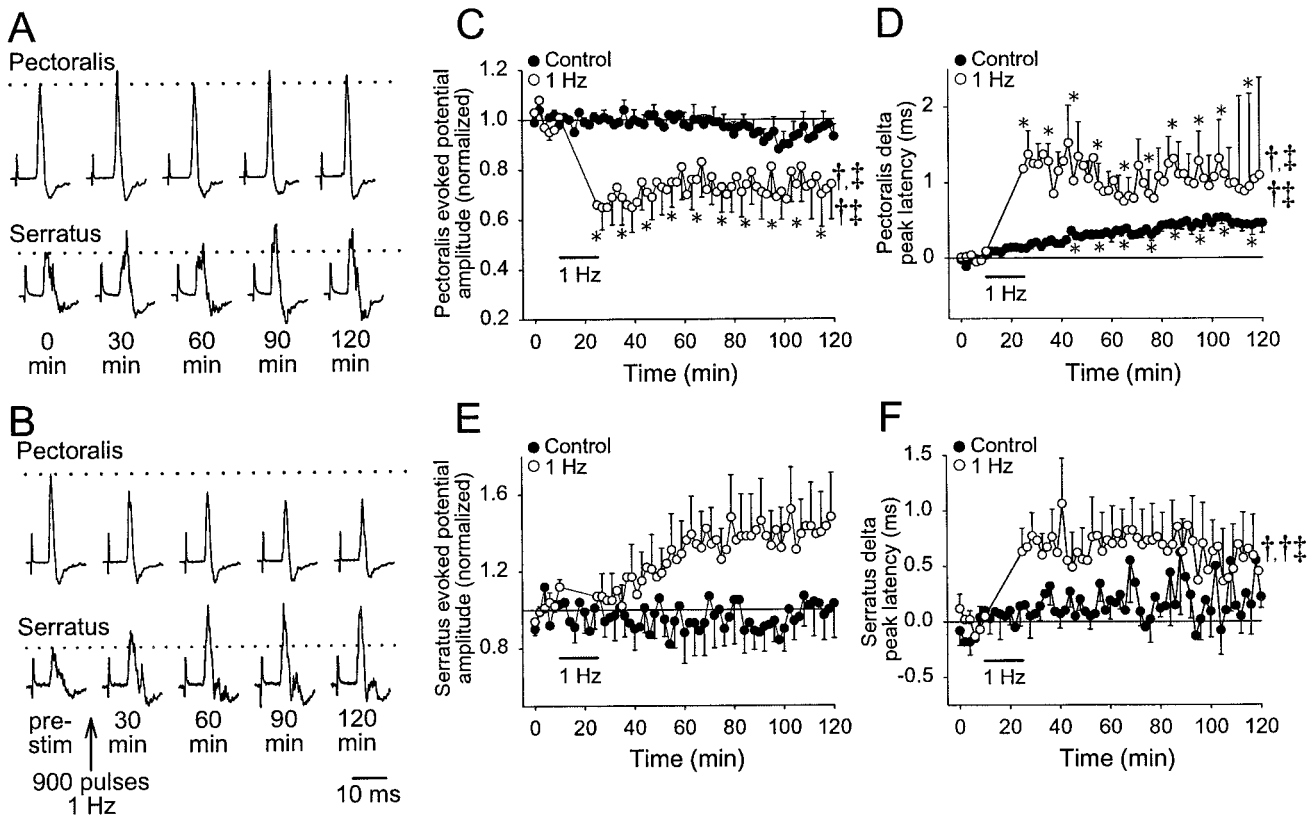
Figure 4. One hertz conditioning stimulation at $[K^+] = 10$ mM. *A*, Sample evoked potentials from a control experiment at various times are shown for pectoralis (*top traces*) and serratus (*bottom traces*). Test stimuli were applied every 2 min for 2 hr. The *dotted line* shows the average amplitude for the traces obtained in the first 10 min, and stimulus artifacts are truncated. *B*, Sample evoked potentials from an experiment in which conditioning stimulation was applied are shown. After 10 min of test stimuli, 1 Hz conditioning stimulation (900 pulses, 0.2 msec duration, 400 μA) was applied at the time indicated by the *arrow*. The change in pectoralis (*C*) and serratus (*E*) evoked potential amplitude with respect to time is shown. The control data, in which only test stimuli were applied, are indicated by *solid circles* ($n = 6$), whereas the data for the conditioned preparations are indicated by *open circles* ($n = 8$). The change in peak latency of pectoralis (*D*) and serratus (*F*) evoked potentials with respect to time is shown. Statistical *symbols* are the same as described in Figure 3.

LTD of pectoralis evoked potential amplitude is frequency-dependent

Given that the most robust response with 1 Hz conditioning stimulation was LTD of pectoralis evoked potential amplitude, we tested whether the amplitude depression was dependent on the frequency of conditioning stimulation. In these experiments, 900 pulses (400 μA, 0.2 msec duration) were applied at 10 Hz ($n = 6$) or 100 Hz ($n = 6$), with the $[K^+]$ in the caudal spinal compartment at 10 mM, except for three 100 Hz and two 10 Hz conditioning stimulation experiments, which were at 7 mM $[K^+]$. Because there were no differences in the results at 7 or 10 mM $[K^+]$, the data were pooled. In addition, control experiments in which test stimuli were applied every 2 min were performed to generate control data for two-way comparisons ($n = 6$). In these control experiments, there were no significant changes in the amplitude or peak latency of pectoralis or serratus evoked potentials (Fig. 5*A–D*).

After 10 Hz conditioning stimulation, pectoralis evoked potential amplitude decreased by 40% initially and then relaxed to a 20% decrease that lasted for at least 60 min ($p < 0.05$; Fig. 5*A*). In addition, pectoralis peak latency increased by 0.4–0.6 msec above baseline for 20 min ($p < 0.05$) before returning to ~0.3 msec above baseline (Fig. 5*B*). For pectoralis amplitude and peak latency, 10 Hz conditioning stimulation produced a response that was significantly different from control experiments through the

effects of time, conditioning stimulation, and a time–conditioning interaction (Fig. 5*A,B*). In contrast, serratus evoked potential amplitude increased by 65% immediately after 10 Hz conditioning stimulation ($p > 0.05$) and then decreased by 10–20% for ~30 min ($p > 0.05$) before gradually returning to baseline levels (Fig. 5*C*). Serratus peak latency increased to 1.5 msec above baseline ($p < 0.05$) and then rapidly decreased to 0.2–0.4 msec above baseline ($p > 0.05$; Fig. 5*D*). After 10 Hz conditioning stimulation, the serratus amplitude response was significantly greater than control experiments via conditioning stimulation and a time–conditioning stimulation interaction. The peak latency response resulted from significant time and time–conditioning stimulation interaction (Fig. 5*C,D*).

After 100 Hz conditioning stimulation, pectoralis evoked potential amplitude was depressed by <20% and returned to baseline within 60 min; the conditioning stimulation and time–conditioning stimulation interaction were significant in comparison with control experiments (Fig. 5*A*). Pectoralis peak latency was not significantly altered (Fig. 5*B*). For serratus, the evoked potential amplitude increased by 40% immediately, returned to near baseline levels for 30 min, and increased steadily during the next 30 min to reach a maximum level 72% above baseline ($p < 0.05$; Fig. 5*C*). The increase in serratus evoked potential amplitude was variable, (i.e., serratus amplitude increased by >20% in only three of six preparations). When compared with control experi-
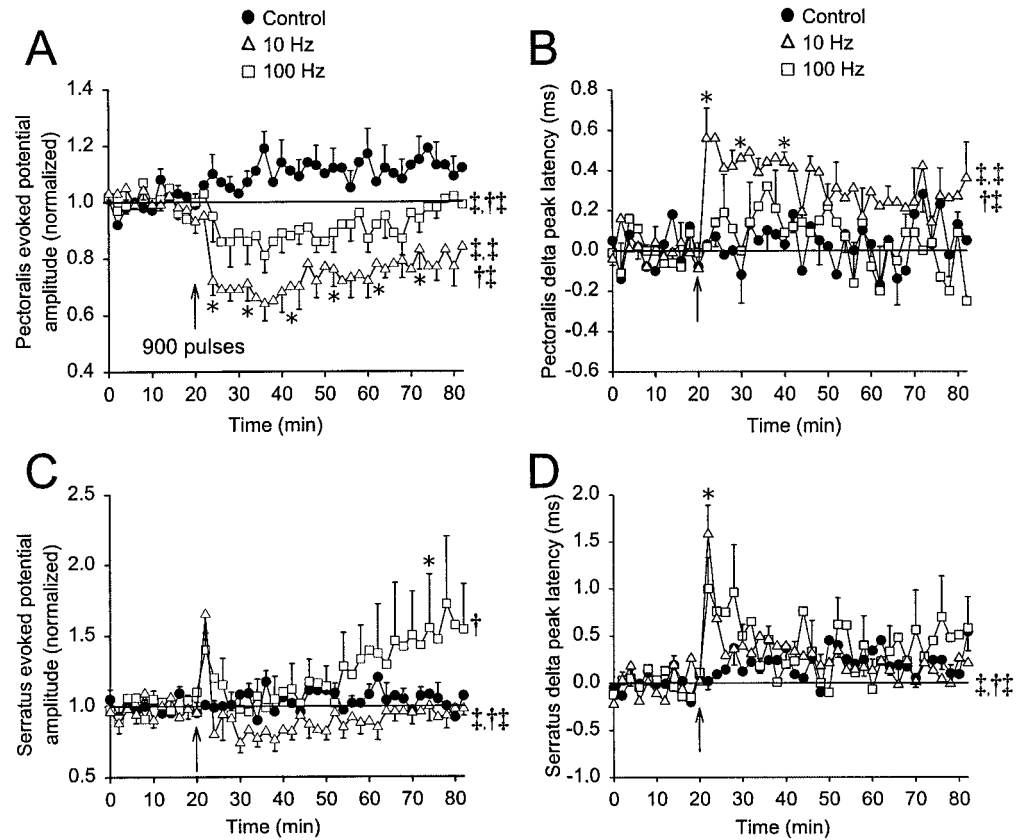
Figure 5. Frequency-dependent effects of conditioning stimulation. The amplitudes of pectoralis (*A*) and serratus (*C*) evoked potentials with respect to time are shown for controls (*closed circles*; *n* = 6, no conditioning stimulation applied) and for the application of conditioning stimulation at 10 Hz (*open triangles*; *n* = 6, 900 pulses) and 100 Hz (*open squares*; *n* = 6, 900 pulses). In four of six preparations, control data were obtained before applying conditioning stimulation. Conditioning stimulation was applied as indicated by the *vertical arrow*. The changes in pectoralis (*B*) and serratus (*D*) peak latency with respect to time are shown with the *symbols* described above. Statistical *symbols* are the same as in Figure 3.

ments, the serratus amplitude response was significantly greater than control because of a time effect. Serratus peak latency increased by 1.0 msec immediately after stimulation and then decreased rapidly to near baseline levels (*p* > 0.05; Fig. 5*D*). Although long-lasting, we cannot define the delayed potentiation in serratus amplitude as LTP, because the potentiation was not demonstrated to last for >1 hr (see introductory remarks).

Sensory afferent evoked potentials in pectoralis express LTD after low-frequency stimulation

To test whether 1 Hz conditioning stimulation applied to the spinal cord altered a different set of synaptic inputs to pectoralis and/or serratus motoneurons, segmental sensory afferent inputs were activated by electrically stimulating the ipsilateral dorsal root at C_8 (*n* = 5). Activation of segmental afferent inputs elicited an evoked potential in pectoralis but not in serratus nerves, even though the caudal spinal compartment [K^+] was 10 mM (Fig. 6*A*). Pectoralis evoked potentials resulting from sensory afferent stimulation were 62% smaller and had peak latencies that were longer than those from spinal stimulation in the same preparation (15.2 ± 2.0 vs 8.3 ± 0.4 msec; *p* < 0.05). The onset of pectoralis evoked potentials after sensory afferent stimulation were also longer than evoked potentials after spinal stimulation (11.1 ± 1.3 vs 5.8 ± 0.2 msec; *p* < 0.05). After obtaining baseline data for 40 min, 10 Hz conditioning stimulation (900 pulses) applied to the spinal cord depressed both descending and sensory afferent evoked potentials (40–50% with a slight return toward baseline levels 80–100 min later; *p* < 0.05; Fig. 6*B*).

DISCUSSION

This is the first study to demonstrate long-lasting, activity-dependent plasticity in descending pathways to spinal motoneu-

rons involved in respiration and locomotion in an adult vertebrate spinal cord preparation. After 1 and 10 Hz conditioning stimulation, pectoralis evoked potential amplitude decreased and peak latency increased for >1 hr. Given that the amplitude and peak latency reflect the degree of synchronized action potential firing within a pool of motoneurons, the decrease in amplitude and increase in peak latency for pectoralis suggest a depression of synaptic transmission and/or motoneuron excitability. In contrast, serratus evoked potential amplitude was not altered significantly after 1 or 10 Hz conditioning stimulation but expressed a delayed potentiation after 100 Hz conditioning stimulation.

General caveats and limitations

One limitation of recording from whole nerves (or field potentials) is that it cannot be determined whether synaptic transmission, motoneuron excitability, or both are altered after conditioning stimulation. The overriding advantages, however, include ease of recording and clear identification of the motoneurons producing the evoked potentials. The large early peak in the evoked potentials may have been monosynaptic, because it was relatively unaffected by conditioning stimulation (10 and 50 Hz; data not shown) with onset times of 4.3–5.0 msec. These onset times correspond to a conduction velocity of 8–11 m/sec (~4 cm from stimulating electrode to recording electrode), which is within the range of 10–20 m/sec for turtle nerves (Ruigrok et al., 1984; Woodbury and Ulinski, 1986). Although these data are consistent with a monosynaptic pathway, more rigorous analysis will be required to demonstrate this relationship conclusively.

Propriospinal neurons activated at C_5 may have also contributed to the pectoralis and serratus evoked potentials (Nakazono and Aoki, 1994). However, in the hindlimb enlargement of turtles,
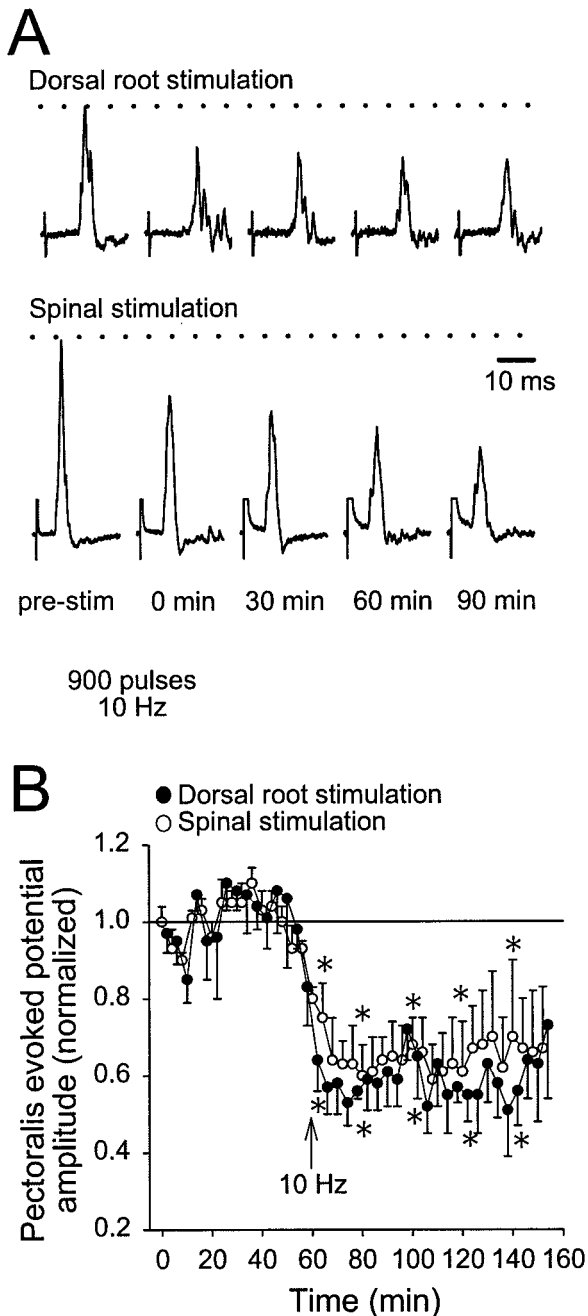
Figure 6. Spinal 10 Hz conditioning stimulation decreased segmental sensory afferent evoked potentials. *A*, With the caudal spinal compartment [K$^+$] at 10 mM, test stimuli were alternately applied every 4 min to either to the dorsal root at C$_8$ or the spinal cord at C$_5$ to produce evoked potentials on pectoralis (*top traces*, dorsal root stimulation; *bottom traces*, C$_5$ spinal cord stimulation). Ten hertz conditioning stimulation applied to the spinal cord at C$_5$ (indicated by the *arrow*) reduced the amplitude of both sets of evoked potentials. Dorsal root stimulation produced no evoked potentials in serratus. *B*, Population data for pectoralis evoked potentials after dorsal root stimulation (*solid circles*) and spinal stimulation (*open circles*; n = 5). Statistical *symbols* are the same as in Figure 3.

descending propriospinal axons typically project to the contralateral spinal cord (Berkowitz and Stein, 1994a,b). Thus, if cervical propriospinal neurons are similarly organized, the contribution of propriospinal neurons to the evoked potentials is expected to be small.

Potential cellular mechanisms underlying LTD in the turtle spinal cord

Although the mechanisms underlying LTD in the turtle spinal cord are not known, important inferences can be made from our data. LTD in pectoralis was heterosynaptic because the amplitude of dorsal root evoked pectoralis potentials was also depressed after conditioning stimulation of the descending spinal pathway. Thus, either pectoralis motoneuron excitability was generally decreased, or a diffusible neuroactive substance was released that produced a widespread inhibition of presynaptic terminals.

In terminals synapsing onto spinal motoneurons, it is possible that vesicle mobilization did not keep pace with release during repetitive stimulation (for review, see Zucker, 1989). Transmitter depletion, however, is not a likely explanation for LTD, because synaptic depression via depletion is greater at high stimulation frequencies (Parker, 1995), and this study demonstrated greater LTD after low-frequency stimulation. Furthermore, if pectoralis LTD was caused by transmitter depletion, then segmental sensory afferent evoked potentials should be unaltered by conditioning stimulation.

Frequency-dependent release of inhibitory neurotransmitters in the spinal cord during conditioning stimulation may produce synaptic depression (Franck et al., 1993), but this is unlikely because pectoralis and serratus motoneurons are in close proximity. Thus, the release of a general inhibitory neurotransmitter (e.g., GABA or glycine) would inhibit both motoneuron pools simultaneously, a prediction not consistent with our results. Furthermore, LTD in pectoralis lasted >115 min, whereas a locally released neurotransmitter might be expected to last only several minutes. Intracellular recordings and extensive pharmacological studies, which are beyond the scope of the present work, will be required to determine the detailed cellular mechanisms underlying LTD in the turtle spinal cord.

Long-lasting, activity-dependent plasticity in the ventral spinal cord

There are few examples of activity-dependent plasticity in descending synaptic inputs to spinal motoneurons. In one study, field potentials in slices of neonatal rat spinal cord expressed LTD, LTP, or no change after stimulation (six bursts of 50 pulses at 100 Hz, separated by 10 sec intervals) of unknown (potentially descending) synaptic inputs to spinal motoneurons (Pockett and Figurov, 1993). In isolated neonatal rat (brainstem)–spinal cord preparations, activation of descending synaptic inputs to spinal motoneurons produced EPSPs that were depressed for an unknown duration or unaltered after short stimulus trains (Elliot and Wallis, 1993; Floeter and Lev-Tov, 1993; Pinco and Lev-Tov, 1994). Thus, activity-dependent plasticity in the spinal ventral horn of neonatal rats has been demonstrated but not systematically investigated with respect to (moto)neuron type, stimulus variables, or the duration of effects.

In contrast, the present study demonstrates long-lasting, stimulus-specific LTD and a delayed potentiation in descending synaptic inputs to (different) identified spinal motoneurons in an isolated adult spinal cord preparation. The delayed potentiation in serratus amplitude is especially noteworthy, because it represents one of the few known examples of long-lasting potentiation in the spinal ventral horn (Pockett and Figurov, 1993; Wolpaw, 1997). It is difficult to directly compare our results with previous work because of the differences in preparations (e.g., reptile vs mammalian, adult vs neonate, and cervical vs lumbar spinal cord) and experimental protocols (e.g., differences in stimulation vari-

ables and location of stimulating electrode). Regardless, our data confirm that activity-dependent plasticity in adult vertebrate spinal cord can be expressed by selected patterns of synaptic activity within a particular pathway.

Plasticity of descending inputs to respiratory spinal motoneurons

Electrical stimulation of descending synaptic inputs to phrenic motoneurons (which project to the diaphragm) in adult rats has been performed, but LTD was not reported (Ling et al., 1994; McCrimmon et al., 1997). A potentially confounding feature in both of those experiments is that 1–2 Hz stimulation was used to study evoked potentials before and during the experiments. Thus, descending synaptic inputs to phrenic motoneurons may have already been depressed. Activity-dependent short-term potentiation (time constant, 49 sec) of descending synaptic inputs to phrenic motoneurons was reported after high-frequency stimulation (100 Hz, 5–60 sec) of the spinal cord in adult, anesthetized rats (McCrimmon et al., 1997). Likewise, in the inspiratory serratus nerve, short-term potentiation occurred after 10 and 100 Hz conditioning stimulation, whereas delayed potentiation occurred after 100 Hz conditioning stimulation. It is possible that synaptic inputs to inspiratory motoneurons in vertebrates are biased toward activity-dependent potentiation versus depression because of the importance of inspiratory movements for survival. Heterogeneity within and between spinal respiratory motoneurons in terms of cellular properties (McCrimmon et al., 1997) and the magnitude of responses during certain forms of plasticity (Fregosi and Mitchell, 1994; McCrimmon et al., 1995; Powell et al., 1998) is likely to be an important property of the respiratory control system.

With regard to breathing, LTD in pectoralis may be used to switch from active expiration to passive expiration when turtles are partially submerged in water. While submerged, water pressure, instead of contracting pectoralis muscles, could be used to push the pectoral girdles inward during expiration. Thus, synaptic depression may represent a strategy for conserving resources, providing for a wider dynamic range when the turtle emerges from the water. In contrast, delayed potentiation may be used to increase (or maintain) tidal volume by increasing the contribution of the pectoral girdle to ventilation, particularly if pelvic girdle movement is compromised by hindlimb injury or when the cloacal bursae and bladder are distended with water during buoyancy regulation (Jackson, 1969).

Plasticity of descending inputs to locomotor spinal motoneurons

Because pectoralis and serratus motoneurons are multifunctional, it is possible that LTD and delayed potentiation may also be expressed in the subset of synaptic inputs that are involved in locomotion. With respect to locomotion, the role of LTD in pectoralis is not clear and requires further investigation, whereas delayed potentiation may compensate for compromised hindlimb movement as described above. If further experiments confirm that LTD and delayed potentiation are expressed at locomotor synapses in the turtle spinal cord, it would add to the growing list of locations in locomotor neural circuitry that express activity-dependent plasticity. For example, long-lasting (>30 min) activity-dependent plasticity is expressed in corticospinal inputs to spinal interneurons (Iriki et al., 1990), afferent inputs to spinal motoneurons (for review, see Wolpaw, 1997) and dorsal horn neurons (for review, see Randic, 1996), and the neuromuscular

junction (Wan and Poo, 1999). Likewise, short-term (<30 min) activity-dependent plasticity in the spinal cord is hypothesized to be an important mechanism regulating the expression of rhythmic locomotor activity in the chick (O'Donovan and Rinzel, 1997; Fedirchuk et al., 1999) and lamprey (Parker and Grillner, 1999). It is well established that spinal plasticity is an important feature of recovery from spinal cord injury (Durkovic, 1986; Hodgson et al., 1994; Muir and Steeves, 1997) (also see Carrier et al., 1997), and it is likely that activity-dependent spinal plasticity is one of several mechanisms contributing to such recovery. Thus, the turtle brainstem–spinal cord preparation might be an ideal preparation for examining the potential role of activity-dependent plasticity of descending inputs to spinal motoneurons.

REFERENCES

Bear MF, Abraham WC (1996) Long-term depression in hippocampus. Annu Rev Neurosci 19:437–462.

Berkowitz A, Stein PSG (1994a) Descending propriospinal axons in the hindlimb enlargement of the red-eared turtle: cells of origin and funicular courses. J Comp Neurol 346:321–336.

Berkowitz A, Stein PSG (1994b) Activity of descending propriospinal axons in the turtle hindlimb enlargement during two forms of fictive scratching: broad tuning to regions of the body surface. J Neurosci 14:5089–5104.

Bliss TVP, Collingridge GL (1993) A synaptic model of memory: long-term potentiation in the hippocampus. Nature 361:31–39.

Carrier L, Brustein E, Rossignol S (1997) Locomotion of the hindlimbs after neurectomy of ankle flexors in intact and spinal cats: model for the study of locomotor plasticity. J Neurophysiol 77:1979–1993.

Durkovic RG (1986) The spinal cord: a simplified system for the study of neural mechanisms of mammalian learning and memory. In: Development and plasticity of the mammalian spinal cord (Goldberger ME, Gorio A, Murray M, eds), pp 149–162. New York: Springer.

Elliot P, Wallis DI (1993) Glutamatergic and non-glutamatergic responses evoked in neonatal rat lumbar motoneurons on stimulation of the lateroventral spinal cord surface. Neuroscience 56:189–197.

Fedirchuk B, Wenner P, Whelan PJ, Ho S, Tabak J, O'Donovan MJ (1999) Spontaneous network activity transiently depresses synaptic transmission in the embryonic chick spinal cord. J Neurosci 19:2102–2112.

Floeter MK, Lev-Tov A (1993) Excitation of lumbar motoneurons by the medial longitudinal fasciculus in the in vitro brain stem spinal cord preparation of the neonatal rat. J Neurophysiol 70:2241–2250.

Franck J, Brodin E, Fried G (1993) Differential release of endogenous 5-hydroxytryptamine, substance P, and neurokinin A from rat ventral spinal cord in potential to electrical stimulation. J Neurochem 61:704–711.

Fregosi RF, Mitchell GS (1994) Long-term facilitation of inspiratory intercostal nerve activity following carotid sinus nerve stimulation in rats. J Physiol (Lond) 477:469–479.

Gans C, Hughes GM (1967) The mechanism of lung ventilation in the tortoise *Testudo graeca linne*. J Exp Biol 47:1–20.

Hodgson JA, Roy RR, de Leon R, Dobkin B, Edgerton VR (1994) Can the mammalian lumbar spinal cord learn a motor task? Med Sci Sports Exerc 26:1491–1297.

Iriki A, Keller A, Pavlides C, Asanuma H (1990) Long-lasting facilitation of pyramidal tract input to spinal interneurons. NeuroReport 1:157–160.

Jackson DC (1969) Buoyancy control in the freshwater turtle, *Pseudemys scripta elegans*. Science 166:1649–1651.

Johnson SM, Mitchell GS (1998a) NMDA-mediated bulbospinal respiratory drive is pH/PCO$_2$-insensitive in turtle brainstem-spinal cord preparation. Respir Physiol 113:201–212.

Johnson SM, Mitchell GS (1998b) Long-term depression is expressed in descending synaptic inputs to respiratory spinal motoneurons in turtles. Soc Neurosci Abstr 23:380.

Linden DJ (1994) Long-term synaptic depression in the mammalian brain. Neuron 12:457–472.

Ling L, Bach KB, Mitchell GS (1994) Serotonin reveals ineffective spinal pathways to contralateral phrenic motoneurons in spinally hemisected rats. Exp Brain Res 101:35–43.

McCrimmon DR, Dekin MS, Mitchell GS (1995) Glutamate, GABA, and serotonin in ventilatory control. In: Regulation of breathing, Vol 79 (Dempsey JA, Pack AI, eds), pp 151–218. New York: Dekker.

McCrimmon DR, Zuperku EJ, Hayashi F, Dogas Z, Hinrichsen CFL, Stuth EA, Tonkovic-Capin M, Krolo M, Hopp FA (1997) Modulation of the synaptic drive to respiratory premotor and motor neurons. Respir Physiol 110:161–176.

Muir GD, Steeves JD (1997) Sensorimotor stimulation to improve loco-motor recovery after spinal cord injury. Trends Neurosci 20:72–77.

Nakazono Y, Aoki M (1994) Excitatory connections between upper cervical inspiratory neurons and phrenic motoneurons in cats. J Appl Physiol 77:679–683.

O'Donovan MJ, Rinzel J (1997) Synaptic depression: a dynamic regula-tor of synaptic communication with varied functional roles. Trends Neurosci 20:431–433.

Parker D (1995) Depression of synaptic connections between identified motor neurons in the locust. J Neurophysiol 74:529–538.

Parker D, Grillner S (1999) Activity-dependent metaplasticity of inhib-itory and excitatory synaptic transmission in the lamprey spinal cord locomotor network. J Neurosci 19:1647–1656.

Pinco M, Lev-Tov A (1994) Synaptic transmission between ventrolateral funiculus axons and lumbar motoneurons in the isolated spinal cord of the neonatal rat. J Neurophysiol 72:2406–2419.

Pockett S, Figurov A (1993) Long-term potentiation and depression in the ventral horn of rat spinal cord in vitro. NeuroReport 4:97–99.

Powell FL, Milsom WK, Mitchell GS (1998) Time domains of the hy-poxic ventilatory response. Respir Physiol 112:123–134.

Randic M (1996) Plasticity of excitatory synaptic transmission in the spinal cord dorsal horn. Prog Brain Res 113:463–506.

Ruigrok TJH, Crowe A, Ten Donkelaar HJ (1984) Morphology of lum-bar motoneurons innervating hindlimb muscles in the turtle *Pseudemys scripta elegans*: an intracellular horseradish peroxidase study. J Comp Neurol 230:413–425.

Stein PSG, McCullough ML, Currie SN (1998) Spinal motor patterns in the turtle. Ann NY Acad Sci 860:142–154.

Takeda R, Remmers JE, Baker JP, Madden KP, Farber JP (1986) Postsynaptic potentials of bulbar respiratory neurons of the turtle. Respir Physiol 64:149–160.

Wan J-J, Poo M-M (1999) Activity-induced potentiation of developing neuromuscular synapses. Science 285:1725–1728.

Wolpaw JR (1997) The complex structure of a simple memory. Trends Neurosci 20:588–594.

Woodbury PB, Ulinski PS (1986) Conduction velocity, size and distri-bution of optic nerve axons in the turtle, *Pseudemys scripta elegans*. Anat Embryol 174:253–263.

Zhuo M, Hawkins RD (1995) Long-term depression: a learning-related type of synaptic plasticity in the mammalian central nervous system. Rev Neurosci 6:259–277.

Zucker RS (1989) Short-term synaptic plasticity. Annu Rev Neurosci 12:13–31.